Metallurgical and Materials Engineering *Research paper*
Association of Metallurgical Engineers of Serbia AMES *https://doi.org/10.30544/827*

FAILURE ANALYSIS OF FRACTURED DENTAL IMPLANTS

Rajesh Bansal[1], Amit Raj Sharma[2], Vakil Singh[3]*

[1]Faculty of Dental Sciences, Institute of Medical Sciences, Banaras Hindu University, Varanasi, Uttar Pradesh, India
[2]All India Institute of Medical Sciences, New Delhi, India
[3]Department of Metallurgical Engineering, Indian Institute of Technology, Banaras Hindu University, Varanasi, Uttar Pradesh, India

Received 19.04.2022
Accepted 14.07.2022

Abstracts

The success and predictability of titanium implants over long periods of time are well established, and there has been a tremendous increase in implant popularity among patients and clinicians over the last four decades. However, complications can occur, resulting in the loss of both, the implant and the prosthesis. Dental implant fracture is uncommon; however, implants or abutment screws can fracture and cause significant problems for both, the clinician and the patient. Improper design, overload, fatigue, and corrosion are all potential causes of implant fracture. Six retrieved fractured dental implants of varying diameter and thread design were collected on a regular basis to characterize their fracture behavior by SEM and assess the fracture mechanism. The majority of the implants were fractured as a result of fatigue crack initiation and propagation from the thread roots.

Key words: fracture; fatigue; dental; implant; fractography; titanium; corrosion.

Introduction

The long-term success and predictability of titanium implants is well established, and there has been a tremendous increase in implant popularity among patients and clinicians over the last four decades [1-3]. Despite their high success rate, varying degrees of dental implant failure have been reported [4-5]. However, the success of implants varies depending on the patient and the location of the implant [6-7]. Failures of osseointegration of dental implants can also be caused by low bone density, a lack of initial stability, bone resorption, cigarette smoking, excessive loading, screw loosening or fracture, and implant fracture [7-12].

*Corresponding author: Rajesh Bansal, *rajeshbansal97@gmail.com*

Dental implants are typically made of commercially pure titanium (CP-Ti), which has a low modulus of elasticity and forms an oxide pellicle on its surface. Because of its superior mechanical properties, they are also made of titanium alloy Ti 6Al 4V; however, V and Al leach out of the alloy Ti 6Al 4V and cause cytotoxicity [13]. Attempts have been made to create vanadium-free beta titanium alloys with a lower modulus of elasticity (closer to bone), high fatigue and corrosion resistance, and improved biocompatibility [14-15]. The fracture behavior of a retrieved CP-Ti dental abutment screw was found to be transgranular, with ductile and fatigue fracture features, as a result of stress corrosion cracking [16].

SEM and TEM were used to examine dental implants and screws; it was discovered that overload caused migration of low angle grain boundaries at fracture surfaces [17]. The fracture surfaces of six CP-Ti dental implants fractured intra orally after an average of 30 months revealed fatigue fracture, with corrosion of the implants being the primary cause [18]. The cause of implant fracture was assumed to be fatigue fracture, with corrosion being the primary underlying factor from long-term use of the dental implant [19]. Another study of seven hollow CP-Ti dental implants that experienced intraoral fracture revealed that the fracture was caused by fatigue [20].

The fracture behavior of six retrieved CP-Ti dental implants with varying diameters and thread types is investigated in this study. This research focuses on characterizing the fracture behavior of retrieved dental implants and investigating the fracture mechanism.

Materials and Methods

Six fractured dental implants were retrieved from various patients in the Faculty of Dental Sciences on a regular basis in order to characterize their fracture. All of the cases had bone resorption up to two uppermost threads. The retrieved implants were cleaned according to the protocol shown in Table 1.

Table 1. Protocol for cleaning of the retrieved dental implants

Pellicle to be removed	Cleaning solution composition	Cleaning duration
Blood/soft tissue	Sodium hypochlorite 3%	<10 min
Organic layer	Acetone	30 min
Inorganic layer	EDTA 17%	As per need

The retrieved fractured implants were immersed in different chemical solutions in a 100 ml glass beaker and cleaned in a specific sequence to remove the various contaminations from the fracture surfaces. During the cleaning process, the beaker was immersed in a hot water ultrasonic bath. Before moving from one solution to another, the specimens were thoroughly rinsed with water and ethyl alcohol [14].

X-ray diffraction (XRD) was used to characterize the phases in the retrieved implants. Rigaku Mini Flex 300 was used to collect XRD data in the range of 30° to 75° at a scan speed of 5°/min using Cu-Kα radiation. The microstructures of the retrieved implants were characterized using optical microscopy. The implants were sectioned longitudinally along their midsection, mechanically polished on emery papers ranging from 1/0 to 4/0, and etched with Kroll's reagent (5% HNO_3, 10% HF, and 85% H_2O). The optical microscope was used to examine their microstructures (Leica DM1750M).

Fracture surface of the retrieved dental implants was examined using Scanning Electron Microscope (FESEM Quanta 200FEG). A 3 mm piece was cut from the fracture end of each retrieved dental implant and cleaned in acetone with an ultrasonic cleaner to remove any particles stuck to the fracture surfaces. To characterize the fracture behavior of these specimens, SEM was used at an operating voltage of 20 kV. Table 2 shows the diameter and thread pitch of the retrieved implants, which are labeled with numbers 1 through 6.

Table 2. Diameter and thread pitch of the different retrieved implants.

Retrieved implant number	Implant Body Diameter (mm)	Thread Pitch (mm)
1.	4.13	1.5
2.	2.19	1.0
3.	2.96	1.3
4.	3.37	0.9
5.	2.75	0.8
6.	3.45	0.8

Results

Figure 1 depicts the macroscopic features of each retrieved fractured implant. All of the retrieved implants are screw-shaped, with varying diameters and thread designs (Table 2). Visual examination of the fracture surfaces of some of the retrieved implants revealed step-like features across the fracture surface.

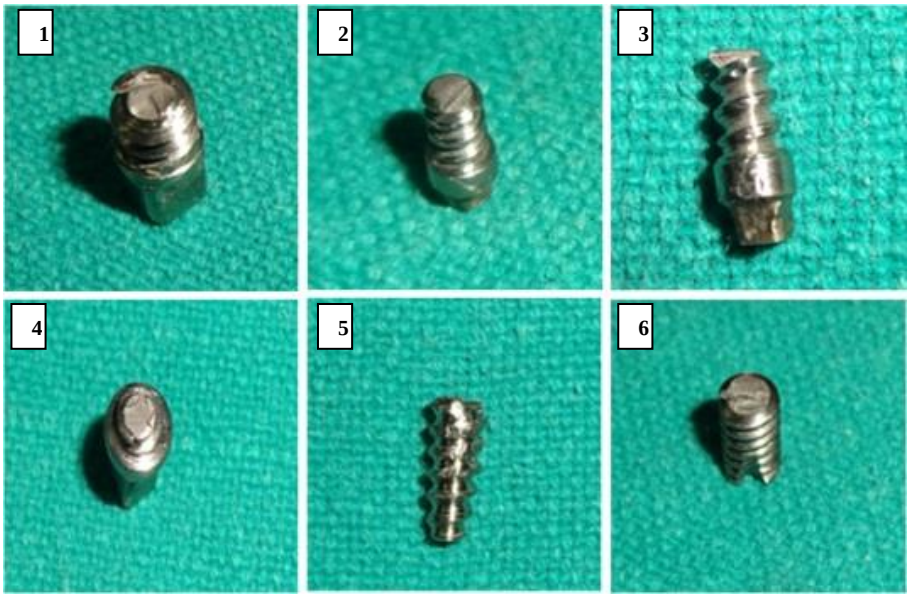

Fig. 1. Macroscopic view of the fractured retrieved implants.

Optical micrographs of the six retrieved implants revealed a single phase microstructure with grain sizes (mean intercept length) ranging from 30, 26, 29, 72, 21, and 42 microns. Figure 2 depicts a representative microstructure of the retrieved implant 4.

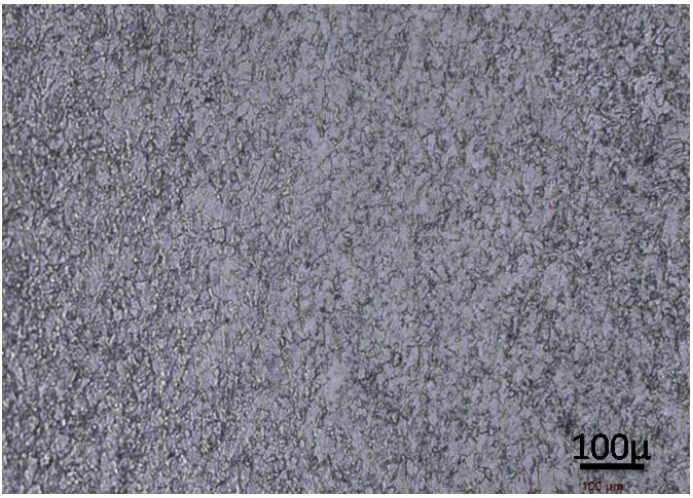

Fig. 2. Optical micrograph of the retrieved implant 4.

Fig.3 shows X-ray diffraction (XRD) profiles of the different fractured implants. It may be seen that there are peaks of essentially α-Ti, along with those of TiO_2 and Ti_2O_3 oxides. Thus, it is obvious that all the six retrieved implants have been of CP-Ti.

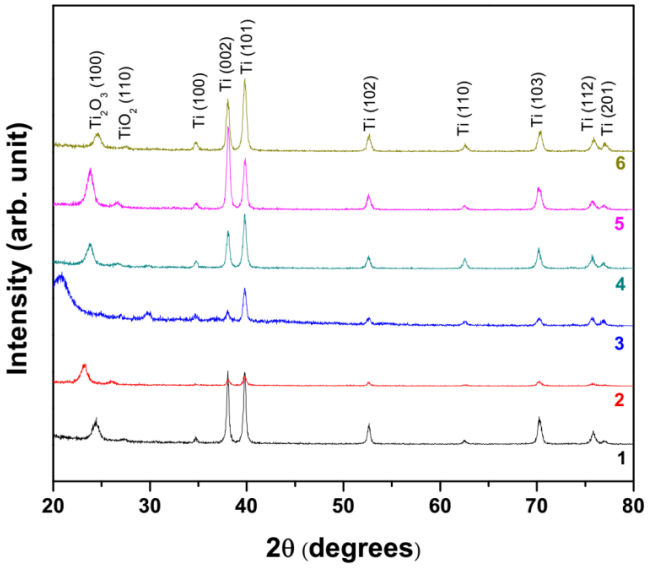

Fig.3. XRD profiles of the different retrieved implants.

SEM was used to examine the fracture characteristics of the six retrieved implants, and their fractographs are shown in Figs 4–9. At low magnification, Fig. 4a depicts a full view of the fracture surface of the retrieved implant 1. The fracture surface is almost flat, and there are a few stepped features on the fracture surface. Cracks were evidently initiated from the thread's root. Figures 4(b) and 4(c) clearly show the initiation and propagation of cracks from the thread root. The stepped region's magnified view reveals distinct fatigue striations (Fig. 4d). The arrow in Fig 4d depicts three closely spaced regions with distinct striations, and the parallel striations are parallel to the arrow's direction.

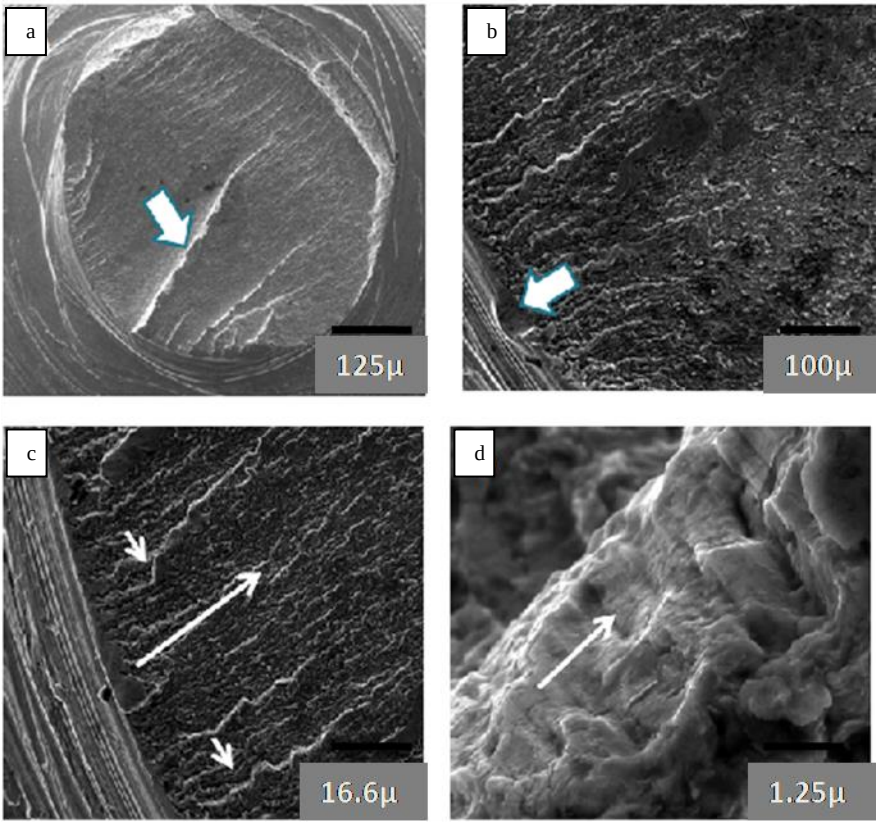

Fig. 4. Scanning electron fractographs of the retrieved implant 1.

Figure 5(a) depicts the fracture surface of the retrieved implant 2 as well as a large step in the central region. An enlarged view of the fracture surface shows crack propagation from the thread's root to the interior (Fig. 5 b); at higher magnification, distinct fatigue striations can be seen. The fracture surface of the retrieved implant 2 (shown in Fig. 5) revealed features similar to that of the retrieved implant 1, with a more prominent step.

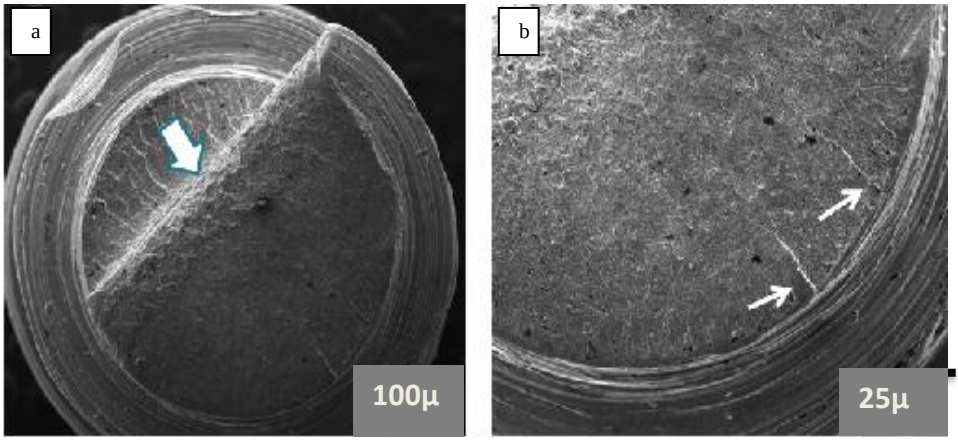

Fig. 5. Scanning electron fractographs of the retrieved implant 2.

Figure 6 depicts the fracture surface of the retrieved implant 3, as well as crack initiation and propagation from the thread root. Fatigue cracks begin at the thread's root and spread to the thread's periphery. Figure 7 depicts the fracture behavior of the retrieved implant 4; different regions of the fracture surface can be seen as a result of crack initiation and propagation. On the right side, the upper region of the fracture surface has distinct fatigue striations.

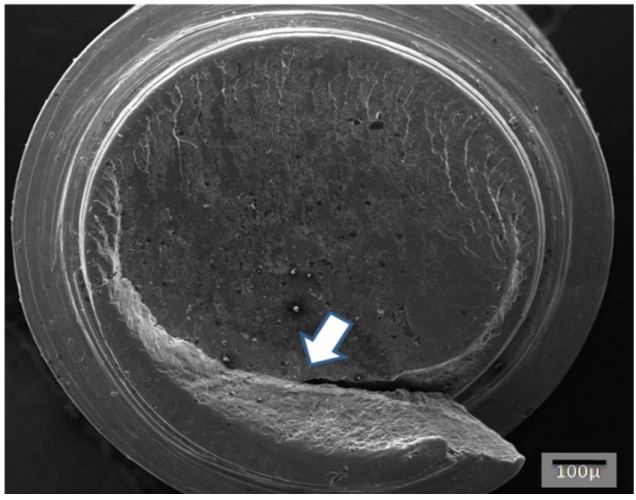

Fig 6. Scanning electron fractograph of the retrieved implant 3.

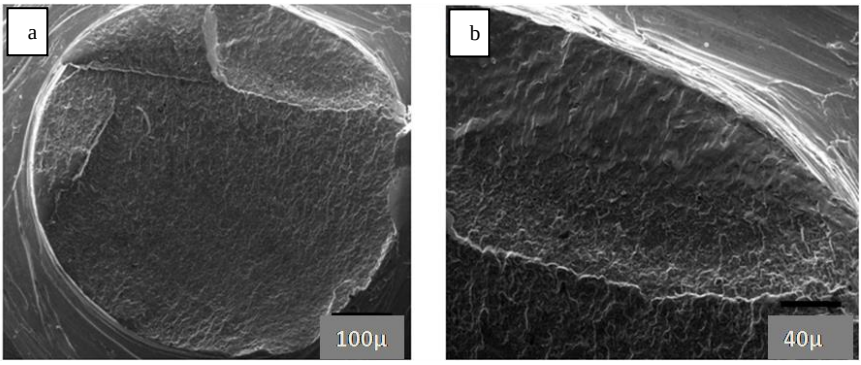

Fig 7. Scanning electron fractograph of the retrieved implant 4.

The fracture surface of retrieved implant 5 is shown in Fig 8, and its features differ significantly from those of the other retrieved implants. It exhibits typical fluted fracture, as seen in titanium and its alloys.

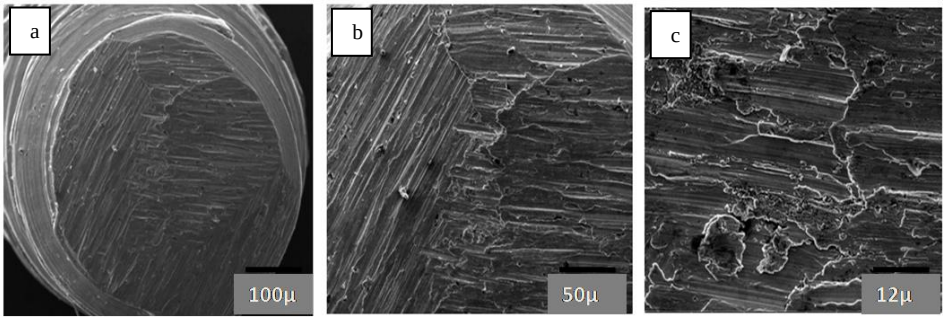

Fig 8. Scanning electron fractographs of the retrieved implant 5.

Figure 9 depicts the fracture surface of the retrieved implant 6. This also demonstrates a distinct step on the fracture surface, similar to the retrieved implants 1-4. The fractograph in Fig 9a shows that the fracture began at the thread root's periphery and spread to the interior. The enlarged view shows the details of the features (Fig 9b, c).

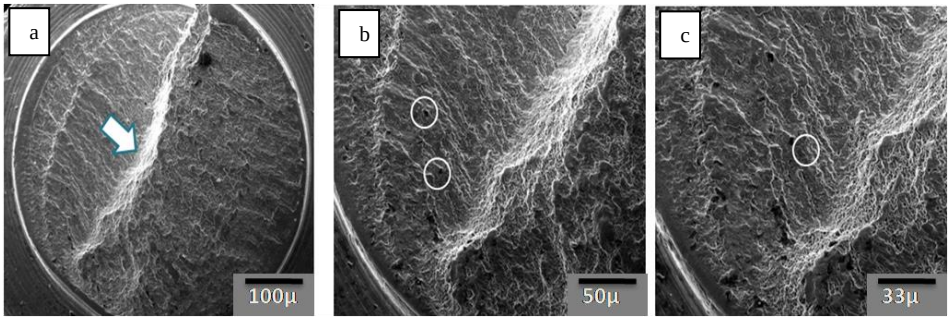

Fig. 9. Scanning electron fractographs of the retrieved implant 6.

Discussion

It is clear that fatigue caused the fracture of the five implants (1, 2, 3, 4, and 6). Fatigue cracks formed at the thread root as a result of stress concentration, propagated inside the implant, and caused implant fracture. The small step-like features along the fracture surface's periphery (Figs. 4, 5, and 6) represent the regions of fatigue crack initiation and initial growth of the fatigue cracks. The level of stress at the implant's thread root is determined by the stress concentration factor (K_t), which is controlled by the sharpness of the thread (root radius) [23-25]. Plastic deformation occurs at the thread root when the stress level exceeds the yield strength of the implant due to cyclic loading of the implant during mastication and biting.

The fracture surface of implant 5 differs significantly from the fracture surfaces of the other implants. The fracture surface has long fluted features, which is a common mode of ductile fracture observed previously in zirconium [26] as well as titanium and its alloys [27-29]. The exact cause of this mode of fracture of implant 5 is unknown; it appears to be associated with localized shearing, possibly as a result of excessive torsional force applied to the implant during its fixing or as a result of couple/torque application during chewing. Dental implant failure has been attributed to a variety of factors, including implant misalignment, poorly taken impressions, peri implantitis and other infections, failed osseointegration, nerve damage, implant failure, foreign body rejection, and allergic reactions [21-22]. One of the reasons for this is implant fracture.

The current work is concerned with analyzing the fracture behavior of six retrieved dental implants in order to determine the mechanism of their fracture. As previously stated, fatigue caused fracture of the five implants (1, 2, 3, 4, and 6); however, it is important to note that features of fracture surfaces of the retrieved dental implants caused by fatigue may differ significantly from those tested in vitro under symmetrical cyclic loading (R=-1). It is because the cyclic load applied to dental implants during mastication and biting does not remain constant, but rather varies with chewing conditions, as with random loading [30]. As a result, depending on the mastication and biting conditions, there may be discontinuity of striations and/or variation in morphology of striations on the fracture surface of dental implants. Further complications arise in the case of dental implants due to the design and roughness of the thread roots [16, 31, 32]. Corrosion of implants is also thought to be a cause of premature fracture of dental implants [18, 33], but it was not discovered to be the cause of fracture of the implants studied in this study. Seeing as data on the service duration of the various implants was unavailable, it was not possible to correlate their performance with their diameters and thread designs.

Conclusion

This study examines the fracture behavior of six retrieved, single stage Cp titanium dental implants with diameters ranging from 2.19 to 4.13mm. Among these, five implants (1, 2, 3, 4, and 6) fractured primarily due to fatigue, while implant 5 fractured possibly due to excessive torsional force applied during implant fixing or due to application of couple/torque during chewing.

References

[1] M. Balazic, J. Kopac, M.Jackson, W.Ahmed: Int J Nano Biomater, 1 (2007) 3-34.
[2] G.A.R. Zarb, A. Schmitt: J.Prosthet. Dent, 64(1990) 185-194.
[3] J.T. Steigenga, K.F. al-Shammari, F.H. Nociti, C.E.Misch, H.L.Wang: Implant. Dent. 12 (2003) 306-17.
[4] P.K. Moy, D. Medina, V. Shetty, T.L. Aghaloo: Int J Oral Maxfac Imp, 20 (2005) 569-577.
[5] B. Friberg, T. Jemt, U. Lekholm: Int. J. Oral Maxfac Impl, 6 (1991) 17-26.
[6] L. Tolstunov: J Oral Implant, 33 (2007) 211-20.
[7] R.A. Jaffin, C.L. Berman: J Periodntol, 62(1991) 2-4.
[8] C.A. Bain, P.K. Moy: Int J Oral Maxfac Impl, 8 (1993) 13.
[9] Y. Manor, S. Oubaid, O. Mardinger, G. Chaushu, J. Nissan: J Oral Maxillofac Surg, 67 (2009) 2649-2652.
[10] A. Piattelli, M. Piattelli, A. Scarano, L. Montesani: Int J Oral Maxillofac Implants, 13 (1998) 561-64.
[11] M.J. Han, C.H. Chung, H.C. Choi: J Korean Acad Prosthodont, 40 (2002) 275- 86.
[12] A. Piattelli, M. Piattelli, A. Scarano, L. Montesani: Int J Oral Maxillofac Implants, 13 (1998) 561-64.
[13] E. Lemons, F. Misch-Dietsh, Biomaterials for dental implants, 3rd ed., In: Misch CE (eds), contemporary implant dentistry, Mosby, St. Louis, 2008, pp 515–17.
[14] R. Van. Noort: J Mater Sci, 22 (1987) 3801–11.
[15] M. Niinomi: Mater Sci Eng A, 243 (1998) 231–6.
[16] K. Yokoyama, T. Ichikawa, H. Murakami, Y. Miyamoto, K. Asaoka: Biomat, 23 (2002) 2459–65.
[17] C.L. Chang, H.K.Lu, K.L. Ou, P.Y. SuY, C.M. Chen: J Dent Sci, 8 (2013) 8-14.
[18] H.C. Choe, J.K. Lee, C.H. Chung: Met Mater Int, 10 (2004) 327–35.
[19] R.W. Kim, H.S. Kim, H. C. Choe, M.K. Son, C.H. Chung: Procedia Eng, 10 (2011) 1955-60.
[20] L. Sbordone, T. Traini, S. Caputi, A. Scarano, C. Bortolaia, A. Piattelli: J Oral Implantol, 36 (2010) 105–112.
[21] W. Chee, S. Jivraj: Br Dent J, 202 (2007) 123-29.
[22] L. Levin: J Appl Oral Sci, 16 (2008) 171-75.
[23] M. B. P. Allery G. Birkbeck: Eng Fract Mechan, 4 (1972) 325-331.
[24] K. Shentov-Yona, Daniel Rittel, Eli E. Machtei, L. Levin: Clin Implant Dent Relat Res, 16 (2014) 178-184.
[25] G. E. Dieter, Mechanical Metallurgy, McGraw Hill Education (India) Edition, 2018,
[26] I. Itchisen, B. Cox: Corrosion, 28 (1972) 83-87.
[27] J. Spurrier, J C. Scully: Corrosion, 28 (1972) 453-63.
[28] C. Ramachandra, V. Singh: Met. Trans A, 16A (1985) 227-31.
[29] J. C. Chestnut, J. C. Williams: Metall Trans A, 8A (1977) 514-15.
[30] K. Shemtov-Yona and D. Rittel: Dental J, 4(2004) 16
[31] D. Novovic, R.C. Dewes, D.K. Aspinwall, W. Voice, P. Bowen: Int J Mach Tool Manu, 44 (2004) 125-34.
[32] M. Aman, Y Tanaka, Y. Murakami, H Remes, G. Marquis: Procedia Struct Integ, 7 (2017) 351-58.
[33] K. Shemtov -Yona. D. Rittel, L. Levin. E. Machtei: Clin Oral Impl Res, 14 (2014) 166-70.